WATER RESOURCES RESEARCH, VOL. 33, NO. 4, PAGES 589–598, APRIL 1997

Field-scale water transport in unsaturated crystalline rock

T. Gimmi,[1] M. Schneebeli,[2] H. Flühler,[1] H. Wydler,[1] and T. Baer[3]

Abstract. Safe disposal of toxic wastes in geologic formations requires minimal water and gas movement in the vicinity of storage areas. Ventilation of repository tunnels or caverns built in solid rock can desaturate the near field up to a distance of meters from the rock surface, even when the surrounding geological formation is saturated and under hydrostatic pressures. A tunnel segment at the Grimsel test site located in the Aare granite of the Bernese Alps (central Switzerland) has been subjected to a resaturation and, subsequently, to a controlled desaturation. Using thermocouple psychrometers (TP) and time domain reflectometry (TDR), the water potentials ψ and water contents θ were measured within the unsaturated granodiorite matrix near the tunnel wall at depths between 0 and 160 cm. During the resaturation the water potentials in the first 30 cm from the rock surface changed within weeks from values of less than -1.5 MPa to near saturation. They returned to the negative initial values during desaturation. The dynamics of this saturation-desaturation regime could be monitored very sensitively using the thermocouple psychrometers. The TDR measurements indicated that water contents changed close to the surface, but at deeper installation depths the observed changes were within the experimental noise. The field-measured data of the desaturation cycle were used to test the predictive capabilities of the hydraulic parameter functions that were derived from the water retention characteristics $\psi(\theta)$ determined in the laboratory. A depth-invariant saturated hydraulic conductivity $k_s = 3.0 \times 10^{-11}$ m s^{-1} was estimated from the $\psi(t)$ data at all measurement depths, using the one-dimensional, unsaturated water flow and transport model HYDRUS [*Vogel et al.*, 1996]. For individual measurement depths, the estimated k_s varied between 9.8×10^{-12} and 6.1×10^{-11} m s^{-1}. The fitted k_s values fell within the range of previously estimated k_s for this location and led to a satisfactory description of the data, even though the model did not include transport of water vapor.

1. Introduction

The emplacement of radioactive waste in suitable geologic formations is one option for final disposal of such toxic substances. Excavating access or storage tunnels for this purpose into a water-saturated granite formation creates new system boundaries at atmospheric conditions. Even the slightest passive ventilation exports some of the humidity and brings air with a moisture deficit into the system. Under such conditions the tunnel wall is an evaporation boundary embracing three different water transport zones or regimes: (1) water vapor diffusion through a stagnant air layer of variable thickness adjacent to the rock surface, (2) vapor diffusion through the gas phase of a desaturated granite layer of a time-dependent thickness, and (3) liquid water flow from the saturated region through the wetter portion of the unsaturated region. Zones (2) and (3) are distinguished on the basis of the dominant process, since vapor and liquid phase transport may occur simultaneously. The rock water potentials within a surface layer of at most a few centimeters are probably controlled directly by the relative humidity of the tunnel atmosphere. Those farther from the surface but still within the unsaturated region reflect the magnitudes of flow resistance to vapor diffusion and to unsaturated liquid flow. At low saturation degrees, vapor diffusion probably exceeds liquid flow, and the desaturated diffusive zone possibly expands into the unsaturated, but still relatively wet region.

Although we used the term diffusion to describe the vapor movement within the rock matrix, this does not imply that this movement is solely due to pure molecular diffusion driven by vapor density gradients. In fact, if a liquid evaporates and if air is not dissolved at the same rate, thermal as well as pressure gradients are created, which can also act as driving forces for vapor transport. In general, however, it is difficult or even impossible to measure the separate flow components.

Shortly after excavation of a tunnel in the unfractured rock and after starting the ventilation, the rock surface looks dry and hydraulically disconnected from the surrounding saturated flow field of the geological formation. Shutting off ventilation will cause resaturation of the unsaturated zone, thus including it in the saturated hydrological circulation again. The occurrence of an unsaturated zone has to be taken into consideration while interpreting underground hydraulic tests, in particular if the tests need to be performed close to the tunnel surface. Possible trapped gas or air pockets may affect the hydraulic regime by diverting the streamlines of the saturated flow field. Finally, incompletely resaturated regions may affect the dissipation of repository generated gases.

Transient changes of the saturation regime can be explored

[1]Soil Physics, Institute of Terrestrial Ecology, Swiss Federal Institute of Technology ETHZ, Zürich, Switzerland.
[2]Swiss Federal Institute of Snow and Avalanche Research, Davos, Switzerland.
[3]Nagra, Wettingen, Switzerland.

Paper number 96WR03974.
0043-1397/97/96WR-03974$09.00

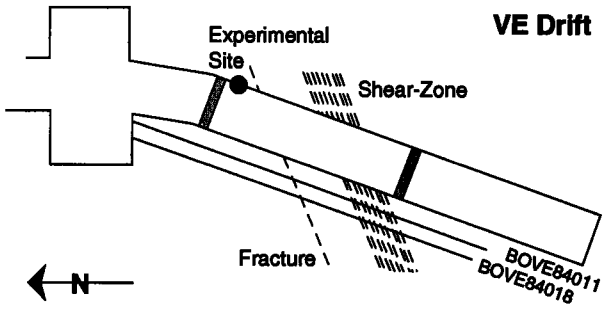

Figure 1. Location of the experimental site within the VE drift of the Grimsel test site (not to scale). The experimental site is separated with a double brick wall from the main tunnel system (to the left) as well as from the rear chamber of the VE drift (to the right).

by means of water flow models. The predictive value of such modeling exercises depends largely on the quality of the parameters used to describe the hydraulic conductivities and specific moisture capacities. With our field experiment we pursued three goals: (1) to provide a database to evaluate various water transport models, (2) to adapt measurement methods developed in the laboratory for applications under realistic field conditions, and (3) to carry out a feasibility study for on-site monitoring of transport processes in the near field of repositories.

2. Material and Methods

2.1. Location

A saturation-desaturation experiment was carried out in a dead-end tunnel 32 m long and 3.5 m in diameter. The tunnel is part of the Grimsel test site (GTS) in the central Swiss Alps, which is operated by the Swiss National Cooperative for the Disposal of Radioactive Waste (Nagra). The experimental area is called Ventilation Drift (VE drift; Figure 1). It is separated from the main tunnel system with a double brick wall at drift meter 448 (i.e., at a horizontal distance of 448 m from the reference location at the entrance of the test site). At drift meter 480 the VE section is divided with another double brick wall into a front and a rear chamber. The instruments were installed approximately at drift meter 450 in the front chamber.

The tunnel system of the Grimsel test site is located 400 m below ground in the central Aare granite. This rock formation includes fairly homogeneous matrix zones as well as pronounced fracture zones, which are separated by meters to tens of meters from each other [*Keusen et al.*, 1989]. At the experimental site the rock matrix is granodiorite with a low cleavage intensity [*Bossart*, 1992]. Within the locked-off experimental section a large fracture zone crosses the tunnel axis between drift meters 465 and 475, and a small fracture cuts at about drift meter 452. Both extend at a mean azimuth of 160°–165° and an angle of about 75° (Figure 1). Since the azimuth of the VE drift is approximately 120°, the small fracture crosses behind our experimental site roughly at a radial distance of 2 m from the tunnel wall.

2.2. Instrumentation

The vapor pressure p_v in terms of the relative humidity, p_v/p_v^0, and the temperature of the air were measured by means of a dew point mirror psychrometer (type Meteolabor VT3), aspiring air in the region between 0 and 5 cm from the rock surface and 2.5 m above the bottom of the tunnel profile. Measurements were taken at 5-min intervals during the saturation phase and at 10-min intervals during the desaturation phase. The readings were averaged to 1- or 6-hour mean values. During the saturation and the desaturation experiment the relative humidity adjacent to the tunnel wall was also measured in a parallel experiment with a capacitive moisture sensor (E. Meier et al., unpublished Nagra report, 1992). This sensor, however, was unreliable at the high relative humidities of the saturation phase, drifting away to readings of more than 1.6 relative humidity.

Seven thermocouple psychrometers (TPs) and four TDR probes were installed radially into the rock for measuring water potential and water content profiles perpendicularly to the tunnel axis (Figure 2). The installation depths of the thermocouple psychrometers were 2 (only during the desaturation experiment), 5, 10, 20, 40, 80, and 160 cm; those for the three-rod TDR probes were 0 (surface probe), 0–30, 30–60, and approximately 60–85 cm, respectively. The construction, measuring principle, and performance of the TP and TDR sensors are described by *Schneebeli et al.* [1995].

The surface TDR probe was glued with an electrically conducting glue directly onto the rock surface. The depth TDR sensors were installed into the granite according to the following procedure. Access boreholes of 117 mm diameter were drilled with a coring bit to the beginning of the installation depths (30 and 60 cm). The cores were broken loose near the front bottom, and the remaining rock pieces were ground flat with a planar diamond disk. The three boreholes for the individual TDR rods were drilled with a 10-mm diamond coring bit. The inside of the coring cylinder was cooled with water at a pressure of 0.7 MPa. For sufficient cooling, pieces of the 5.7-mm-diameter inner core were removed repeatedly from inside the drilling cylinder. The boreholes were cleaned with a water jet and afterwards with compressed air. To avoid air gaps between rods and rock, the inside was coated with a thin film of electrically conducting silicon grease containing silver (trade name Elecolit). The three copper rods were inserted one by one as described by *Schneebeli et al.* [1995]. They protruded about 20 mm from the planar bottom of the access borehole. The inner surfaces of the access boreholes were sealed with

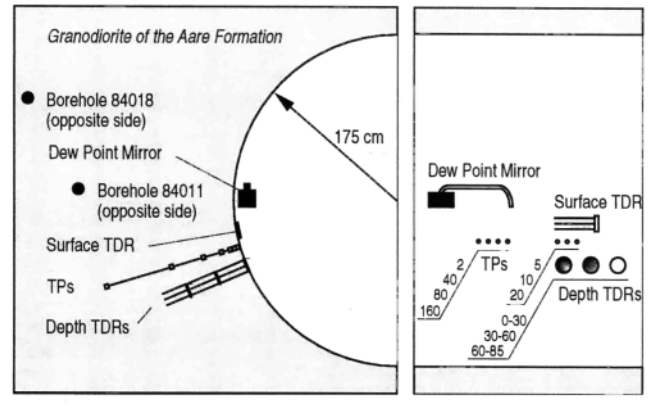

Figure 2. Schematic view of the instrumentation at the experimental site (not to scale). Left-hand side: cross-sectional view. Right-hand side: plan view, with the installation depths given in centimeters. TPs, thermocouple psychrometers; TDR, time-domain reflectometry probe.

Sika Primer 1, a silicon-based commercial sealing compound. Finally, a connector head with three plugs was pushed over the protruding rods.

The thermocouple psychrometers were installed as described by *Schneebeli et al.* [1995]. An additional problem was the coring to depths of more than 40 cm. The corer could be advanced only in short steps, and the drilling device had to be mounted in a very firm and well-guided position to avoid rotational moments and vibrations.

Thermocouple psychrometer and TDR measurements were taken manually in irregular intervals. The TDR traces were recorded with a Tektronix 1502B cable tester and a Macintosh computer and digitally evaluated as described by *Schneebeli et al.* [1995].

Opposite to our experimental site, two boreholes were located parallel to the VE drift (see Figures 1 and 2), at a radial distance of about 1.70 m (BOVE 84011) and 3.5 m (BOVE 84018) from the drift wall. These boreholes were packed at several locations, and the hydraulic heads of the sections were measured with pressure transducers suited for positive heads (H. Kull and I.-M. Planeck, unpublished Nagra reports, 1992, 1993). Sections 84011/5 and 84018/4, each 13 m long, were located directly opposite the experimental site.

2.3. TDR Sensitivities

Using the composite dielectric approach of *Roth et al.* [1990], the composite dielectric number ε_c of a three-component medium like rock depends on the volumetric water content θ according to

$$\varepsilon_c = (\theta\varepsilon_w^\alpha + (1 - \eta)\varepsilon_s^\alpha + (\eta - \theta)\varepsilon_a^\alpha)^{1/\alpha} \quad (1)$$

where ε_w, ε_s, and ε_a are the dielectric numbers of water, solid, and air, respectively; η is the porosity; and α is a geometry parameter with a value of 0.5 for fairly isotropic media. From the travel time t^* of the electromagnetic pulse through the TDR probe, ε_c was evaluated as

$$\varepsilon_c = \left(\frac{t^* - t_0}{2L}\right)^2 c_0^2 \quad (2)$$

where t_0 is the offset of the travel time caused by the passage through the probe head, such that $t = t^* - t_0$ is the net travel time forth and back along the TDR rods of length L, and c_0 is the velocity of light in vacuum (0.2998 m ns^{-1}). From (1) and (2) the sensitivities of the evaluated water content θ on the dielectric constant of the rock ε_s as well as on probe-specific properties like the length L and the offset t_0 were calculated as

$$\frac{\partial\theta}{\partial\varepsilon_s} = (\eta - 1)\frac{\alpha}{(\varepsilon_w^\alpha - \varepsilon_a^\alpha)}\varepsilon_s^{\alpha-1} \quad (3)$$

$$\frac{\partial\theta}{\partial L} = \left(-\frac{2}{L}\right)\frac{\alpha}{(\varepsilon_w^\alpha - \varepsilon_a^\alpha)}\varepsilon_c^\alpha \quad (4)$$

$$\frac{\partial\theta}{\partial t_0} = \left(-\frac{2}{t}\right)\frac{\alpha}{(\varepsilon_w^\alpha - \varepsilon_a^\alpha)}\varepsilon_c^\alpha \quad (5)$$

To estimate the influence of parameter uncertainties, we used, as an example, the following parameter set: $\varepsilon_s = 6.0 \pm 0.5$, $\varepsilon_w = 80$, $\varepsilon_a = 1$, $\alpha = 0.5$, $\eta = 0.01$, $\theta = 0.005$, L $= 0.300 \pm 0.003$ m, and $t_0 = 0.30 \pm 0.05$ ns. This leads to $\varepsilon_c = 6.124$ and $t = 4.953$ ns. The uncertainties of θ then become

$$\delta\theta|_{\varepsilon_s} := \frac{\partial\theta}{\partial\varepsilon_s}\delta\varepsilon_s = \pm 0.013 \quad (6)$$

$$\delta\theta|_L := \frac{\partial\theta}{\partial L}\delta L = \pm 0.0031 \quad (7)$$

$$\delta\theta|_{t_0} := \frac{\partial\theta}{\partial t_0}\delta t_0 = \pm 0.0031 \quad (8)$$

where $\delta\varepsilon_s$, δL, and δt_0 are the assumed uncertainties in each parameter. We see clearly that the estimated uncertainties of θ are of the order of the assumed water content, $\theta = 0.005$, or even the assumed porosity, $\eta = 0.01$. Therefore absolute water contents determined by means of TDR are very uncertain in a medium with such a low porosity like granodiorite.

On the other hand, changes in water content, $\Delta\theta$, can be estimated from changes in the dielectric constant ε_c. This was done using average slopes $\Delta\theta/\Delta\varepsilon_c$ obtained from laboratory calibrations ($\Delta\theta/\Delta\varepsilon_c = 0.0264$ for the depth probes and 0.0326 for the surface probe [*Schneebeli et al.*, 1995]). The estimated changes in water content are less sensitive to systematic errors caused by the imprecisely known local parameters for each probe, but they are still influenced by the random errors of each measurement. Assuming uncorrelated errors, the standard deviation of $\Delta\theta$ is related to the standard deviation of the θ measurements by $\sigma_{\Delta\theta} = 2^{1/2}\sigma_\theta$. The value of σ_θ can be estimated in two ways: (1) from repeated measurements of ε_c at a given water content, with a known relation between ε_c and θ, or (2) from the value of χ^2 of a regression between ε_c and θ, provided a suitable regression model is applied. Using the data of the laboratory calibrations of *Schneebeli et al.* [1995], method 1 led for depth and surface probes to $\sigma_{\Delta\theta}$ between 1.4×10^{-4} and 9.5×10^{-4}, depending on the water content. With method 2, $\sigma_{\Delta\theta}$ was estimated to be 5.5×10^{-4} for the surface probe and 1.4×10^{-3} for the depth probe. The relatively high value of 1.4×10^{-3} for the depth probe certainly overestimates the random errors of single measurements. The dependence of ε_c on θ was not linear over the whole data range for this probe, leading to systematic deviations between the linear regression and the data and thus to a relatively large χ^2 value. Ignoring this last value, the laboratory measurements with both types of probes indicated a $\sigma_{\Delta\theta}$ lower than about 0.001. During the saturation phase of the field experiment, the use of partly unreliable coaxial switches may have increased the noise of the TDR signals and therefore also the value of $\sigma_{\Delta\theta}$.

2.4. Saturation Experiment

The symbol t_s denotes the time during the saturation phase. Prior to the saturation experiment, the drift was ventilated, with some interruptions, for several months. At the end of this preparation phase, several full sets of measurements were taken to document the initial conditions. At $t_s = 0$ (March 5, 1991) the ventilation in the VE drift was shut off. Within three hours free water seeped out of the small fracture that is about 2 m to the right of the nearest sensor. At $t_s = 9$ days a steam vaporizer was installed to increase the air humidity in the enclosed tunnel section. At $t_s = 153$ days the steam vaporizer was disconnected and the site remained enclosed and unventilated for 113 days. All TPs as well as the depth TDR probes were removed at the end of the saturation experiment.

2.5. Desaturation Experiment

We recalibrated the TPs and reinstalled them as well as the depth TDR probes in the same boreholes. An additional TP

was installed at a depth of 2 cm. The TDR coaxial switches, which were used during the saturation experiment, were replaced by ordinary coaxial connectors. We will use the symbol t_d to denote the time during desaturation. At time $t_d = 0$ (November 26, 1991; $t_s = 266$ days), the ventilation was turned on and regulated to keep the relative humidity at about 0.7.

2.6. Modeling

Most models used for describing unsaturated water transport require two nonlinear parameter functions, the unsaturated hydraulic conductivity, $k(\psi)$, and the specific moisture capacity, $C(\psi) = d\theta/d\psi$, where ψ is the water potential. Both $k(\psi)$ and $C(\psi)$ are either unknown, difficult to measure, or unreliable to estimate from indirect experimental observations such as, for instance, the pore size distribution. Today it is a widely accepted, but hardly ever validated, approach to estimate these functions from the moisture retention curve data $\theta(\psi)$, which are in most cases obtained from relatively small samples under laboratory conditions.

The relations $\theta(\psi)$ and $k(\psi)$ are often parameterized using functions proposed by *van Genuchten* [1980] and *Mualem* [1976], which we will refer to as the VG model:

$$\theta(\psi) = \theta_r + (\theta_s - \theta_r)(1 + |\alpha\psi|^n)^{-m} \tag{9}$$

and

$$k(\psi) = k_s s_e^{\tau}[1 - (1 - s_e^{1/m})^m]^2, \tag{10}$$

where θ_r is the residual and θ_s the saturated water content, α is the inverse of the air-entry value, n is a pore size distribution index, $m = 1 - 1/n$, k_s is the conductivity at saturation, τ is an empirical constant usually set equal to 0.5, and s_e is the relative water saturation

$$s_e = \frac{\theta - \theta_r}{\theta_s - \theta_r}. \tag{11}$$

We fitted (9) to the $\theta(\psi)$ data of granodiorite samples that have been reported by *Schneebeli et al.* [1995]. From this fit (shown in Figure 7) we obtained $C(\psi)$ and the relative hydraulic conductivity, $k_r(\psi) = k(\psi)/k_s$, according to (10). The saturated hydraulic conductivity k_s of granodiorite was, as will be shown below, estimated from a part of the data of the desaturation field experiment. Transient water flow calculations for the desaturation phase were performed with the code HYDRUS 5.0 [*Vogel et al.*, 1996], a single-phase, one-dimensional unsaturated water flow and transport model based on the following form of the Richards equation

$$\frac{\partial\theta}{\partial t} = \frac{\partial}{\partial z}\left(\frac{k_s k_r(\psi)}{\rho_w g}\frac{\partial\psi}{\partial z}\right) - \frac{\partial}{\partial z} k_s k_r(\psi)\cos\gamma, \tag{12}$$

where t is time, z is the distance in flow direction, and γ is the angle between the flow direction and the vertical axis. The term $\psi/(\rho_w g)$ equals the hydraulic head h, with ρ_w being the density of water and g being the gravitational acceleration. In our system, gravitation acts more or less perpendicularly to the radial depth coordinate. Compared to the gradients of the matrix potential along the measurement axis, gravitation has little effect near the tunnel wall. The gravitation term in the Richards equation was therefore neglected by assuming $\gamma = 90°$.

The modeled domain from the tunnel surface at 0 cm to a distance of 400 cm was discretized into a total of 112 elements, with sizes ranging from 0.5 mm near the tunnel wall to 10 cm at larger depth. For all depths the estimated VG functions $\theta(\psi)$ and $k_r(\psi)$ were used as input parameters, assuming a homogeneous medium. The water potential in the drift atmosphere was calculated from the measured relative humidity p_v/p_v^0 according to the Kelvin equation [*Rawlins and Campbell*, 1986]

$$\psi = \frac{\rho_w RT}{M_w} ln(p_v/p_v^0), \tag{13}$$

where R is the universal gas constant, T is the absolute temperature, and M_w is the molecular mass of water. This ψ value as well as the water potential observed in the borehole section 84018/4 opposite to the experimental site served as inner and outer boundary conditions. The initial condition was defined by the water potentials measured with the TPs just prior to the start of the desaturation.

A depth-invariant saturated hydraulic conductivity, k_s, was then estimated to match observed and calculated water potentials at all depths. The fitting was performed using a Levenberg-Marquardt algorithm [*Press et al.*, 1992] to minimize the sum of squared deviations between observed and calculated water potentials, which should lead to maximum likelihood estimates in case of independent, normally distributed measurement errors. In a second series of runs, k_s as well as the VG parameters α and n were estimated simultaneously from the water potentials measured in the field.

3. Results and Discussion

3.1. Evaporation Boundary

Within a few hours after stopping the ventilation and shutting off the VE drift from the main tunnel system, the relative humidity increased and reached values of over 0.9 (Figure 3a). Afterwards, the increase slowed down. During the additional humidification with the steam vaporizer, most surfaces exposed to the tunnel air were dripping wet. Based on the relative humidities obtained with the dew point mirror, however, the drift atmosphere did not reach full saturation. The measured potential of the water vapor was consistently below −1.3 MPa ($p_v/p_v^0 < 0.99$), with the exception of the final period of the saturation experiment ($t_s > 105$ d). The readings exceeding a relative humidity of 1.0 were in this case most likely a maintenance problem of the dew point mirror in the very humid environment.

During the desaturation experiment, the short-term variations of the 1-hour averages were larger than those during the saturation experiment (Figure 3b). This was probably due to the cyclic ventilation control at the test site, whereas additional daily cycles were caused by the experimental activities. The sudden changes in the humidity (e.g., $t_d = 10$, 60, and 80 days) coincide with technical problems of the air-conditioning control. The parallel, but independent, humidity measurements by E. Meier et al. (unpublished Nagra report, 1992) indicate that the observed oscillations and long-term trends were real. For describing the water transport through the unsaturated zone, the long-term trends of the relative humidity are important, whereas the higher-frequency fluctuations of the water potential at the boundary are probably damped out within a few centimeters from the rock surface.

3.2. Air and Rock Temperature

Initially, the air temperature was 13.5°C. During the saturation it gradually rose to about 14°C and then dropped back to

13.4°C. During the desaturation experiment the air temperature was generally lower: initially around 12.4°C with a maximum of 13.5°C at t_d = 80 days. Toward the end of the experiment, during the period with ventilation control problems, it dropped down to 12.0°C. The daily temperature oscillations were generally less than ±0.15°C, and the standard deviation of the hourly values was below 0.04°C. In general, the rock temperatures were slightly lower than the air temperature. The temperature gradient between the thermocouple psychrometers at 5 and at 80 cm was usually lower than 0.3°C m^{-1}. This is a fairly isothermal regime, but even such small differences may interfere with the thermocouple psychrometer measurements.

3.3. Water Potentials

Figure 4 shows the water potentials measured with the thermocouple psychrometers as a function of t_s and t_d. The amplitudes of the fluctuations of the TP readings at depths 2 and 5 cm are greater than those at larger depths. During the saturation experiment the water potentials at 5 cm depth increased within 40 days from the initial value of −2.2 MPa to −1.5 MPa. At this time this sensor failed and was removed and replaced. Apparently, the measuring cavity became exposed to the tunnel air of a relative humidity $p_v/p_v^0 \approx 0.97$ (−4 MPa) and dried out somewhat, which interrupted and delayed the saturation. The replaced sensor had a sensitivity about six times lower than the original one. This explains why the standard deviation became much larger after the replacement.

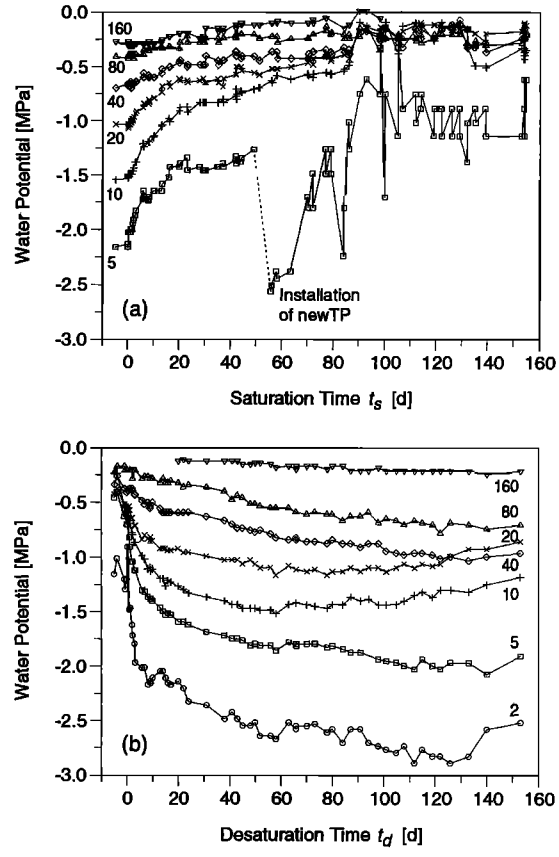

Figure 4. Changes in water potentials measured with thermocouple psychrometers at indicated depths (in centimeters) during (a) the saturation experiment and (b) the desaturation experiment. The measurement uncertainties were about ±0.03 MPa, the upper measurement limit was about −0.1 MPa.

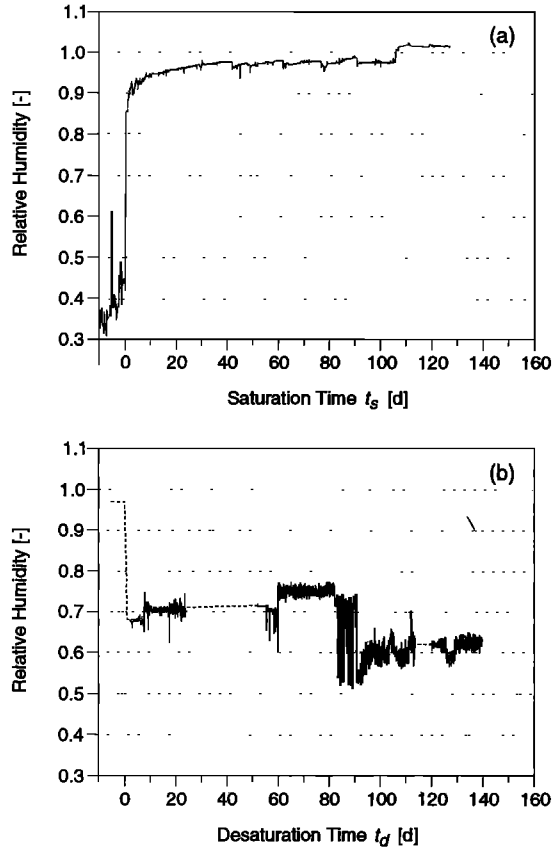

Figure 3. Relative air humidity measured at the experimental site during (a) the saturation experiment and (b) the desaturation experiment (1-hour mean values). Dashed lines are interpolations based on data of E. Meier et al. (unpublished Nagra report, 1992).

After recalibration and reinstallation of all thermocouple psychrometers at the beginning of the desaturation phase (Figure 4b), the water potentials ranged between −0.2 MPa (80 cm), −0.6 MPa (5 cm), and −0.9 MPa (2 cm). These values were in the same range or slightly lower than those observed at the end of the saturation measurements (t_s = 155 days). The TP at 2 cm responded quickly to the resumed ventilation. After 10 days the water potential at 80 cm started to decrease, whereas at 160 cm it took 50 to 60 days before a significant change became detectable.

During both the saturation and desaturation experiment the TP at 160 cm was apparently always functional except for t_s > 90 days. At water potentials approaching zero the thermocouple psychrometer readings are unstable and unreliable. Therefore no measurements were taken at 160 cm for t_s > 100 days and for t_d < 20 days. Since the upper limit for the TP measurements is approximately −0.1 MPa, it cannot be stated whether or not zero or even slightly positive potentials occurred at 160 cm for t_s > 90 days or t_d < 40 days. Below the upper limit the measurement uncertainties of the TP readings were in the order of ±0.03 MPa (about ±0.1 μV).

These data show that during ventilation, in the entire measuring region the water pressures dropped below atmospheric, which defines the gauge pressure. No general conclusion, however, can be drawn about the water saturation at slightly neg-

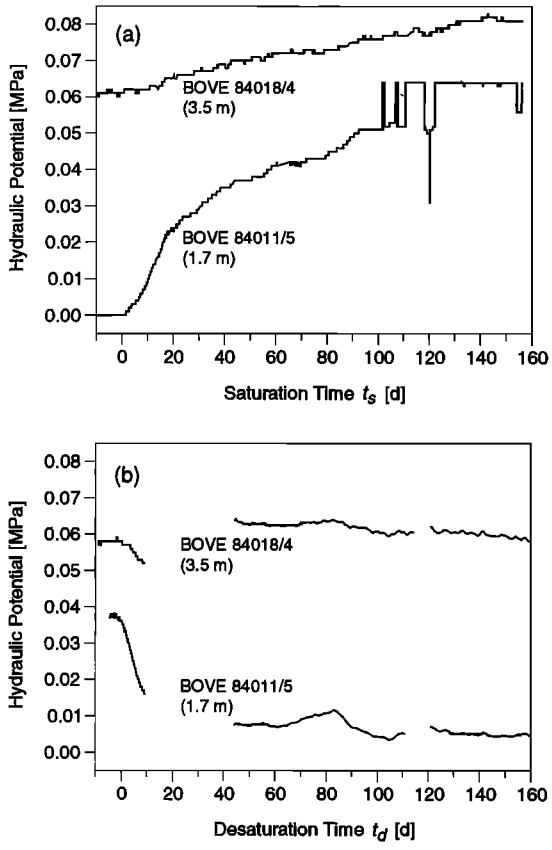

Figure 5. Development of hydraulic heads in packed sections of two boreholes opposite to the experimental site, at a radial distance of 1.7 or 3.5 m. (a) saturation experiment and (b) desaturation experiment. Data from H. Kull and I.-M. Planek (unpublished Nagra reports, 1992, 1993).

ative pressures, unless the shape of the water retention curve near saturation or the air-entry value of granodiorite, respectively, is known. We will address this question in the following paragraphs.

At the end of the drying cycle the water potentials measured at the 40 and 80 cm depths reached lower values than measured before saturation. Those at depths of 10 and 20 cm indicated that temporary and locally, the water potentials may be dominated by other effects than the relative humidity at the tunnel surface. It is not clear to us what caused the increase of the water potentials for $t_d > 120$ days at these locations.

3.4. Zero Pressure Front

The evaporation boundary at the rock surface controls the advancement and recession of the "saturation front," which at this point should be called more cautiously the "zero pressure front" (see section on water contents). Prior to the saturation experiment, the zero pressure front at the experimental site was located somewhere beyond a depth of 1.6 m, possibly influenced by the small fracture appearing 2 m to the right. At a distance of about 1.7 m from the rock surface, but on the opposite side of the VE drift and thus farther apart from the fracture zones, the packed piezometer 84011/5 showed initially no positive pressure (Figure 5), whereas at a distance of 3.5 m (piezometer 84018/4) the pressure was approximately 0.06 MPa (H. Kull and I.-M. Planek, unpublished Nagra report, 1992). The zero pressure front had advanced towards the drift surface to a depth <1.7 m already shortly after shutting off the drift and receded again to somewhere around 1.7 m for $t_d >$ 40 days.

3.5. Water Contents

The composite dielectric numbers ε_c determined during the saturation and desaturation phase are depicted in Figure 6. Except for the surface probe, the temporal variations of ε_c were relatively small. In general, the differences in ε_c between different depth probes or between the two phases of the experiment were larger than the usual scatter of a single probe, which indicates that these individual differences were possibly caused by installation effects, and not necessarily by different absolute water contents.

In Figure 6 the axis on the right-hand side shows the calculated $\Delta\theta$, that is, the differences between the actual and the initial volumetric water content. During the saturation phase the calculated $\Delta\theta$ were rather erratic, with a slight trend towards higher values. The scatter may have been caused partially by the coaxial switches, which were eliminated later. It is difficult to judge whether the relatively large $\Delta\theta$ determined at

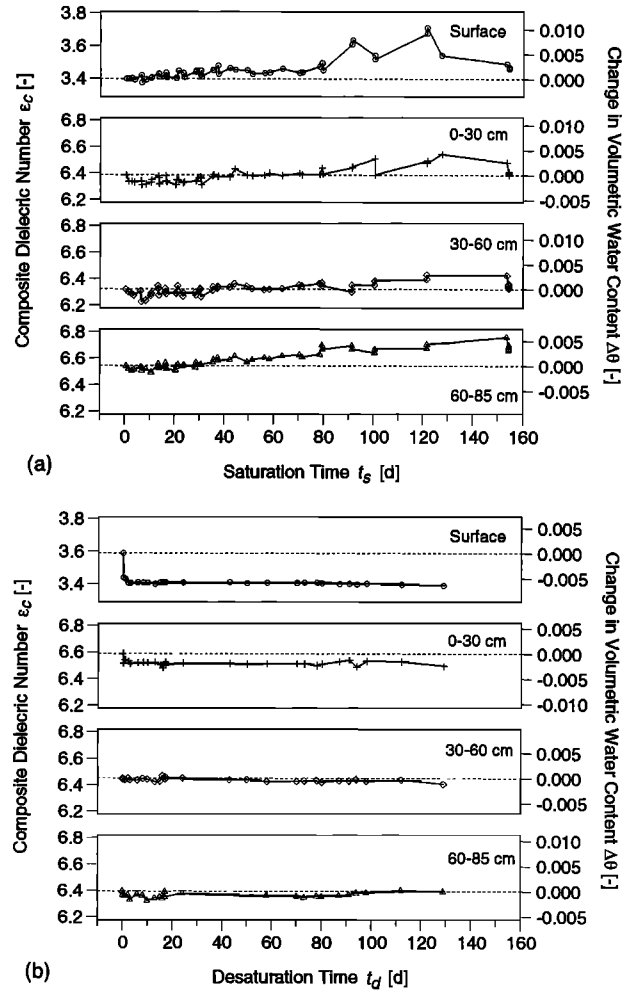

Figure 6. Changes in the composite dielectric number determined with the surface and the depth TDR probes during (a) the saturation experiment and (b) the desaturation experiment. On the right ordinate the corresponding differences between actual and initial volumetric water content, $\Delta\theta$, are given. See section 2.3 for measurement uncertainties.

the surface and at 60–85 cm represent an actual increase of rock water contents. At the surface, direct condensation of water on the waveguides attached onto the rock matrix could have influenced the measurements as well.

During the desaturation phase the behavior of the surface and the depth probes was different. The surface probe showed a rather rapid and distinct decrease during the first 3 days followed by only very slight changes afterwards. The depth probes at 30–60 cm and at 60–85 cm remained essentially in the range of usual scatter for the whole period, with a maximum difference $\Delta\theta$ of about -0.001 to -0.002. The depth probe extending from 0 to 30 cm exhibited a slight decrease during the first 10 days and finally reached a $\Delta\theta$ of about -0.002 to -0.003. The fact that the surface probe was installed perpendicularly to the direction of water flow, but all depth probes were parallel, may partially explain the different responses. The sphere of influence of the probes is not exactly known. It can be assumed that in case of the three-electrode surface probe, the response is dominated by the first few millimeters to centimeters of rock. This area dried out very quickly, as could be inferred from the color of the tunnel surface. Therefore, a rapid response at the surface is plausible. The depth probes, on the other hand, extended over 25 or 30 cm parallel to the water flow. In this case, sudden changes were not expected.

3.6. Water Transport

The water retention data of granodiorite samples as well as the fitted van Genuchten function are shown in Figure 7. The data show two regions where water contents change significantly, which indicates a bimodal pore size distribution. Only with a multimodal water retention function like the one proposed by *Durner* [1994] would it be possible to handle such retention data satisfactorily. *Schneebeli et al.* [1995], however, considered the observed desaturation in the pressure range from -0.1 to -0.5 kPa as an artifact due to surface water on the samples. The mentioned pressure range would correspond to pores with equivalent diameters of 3.0 to 0.6 mm. Such pores were definitively not visible on the sample surfaces. Therefore we ignored this part of the water retention curve by fixing the saturated water content θ_s at 0.0069. With the restrictions $\theta_r = 0$ and $m = 1 - 1/n$, the parameters $\alpha = 1.13$ MPa^{-1} and $n = 1.77$ led to a good fit of the retention data at water potentials below -10 kPa, that is, in the range of water potentials observed in the field.

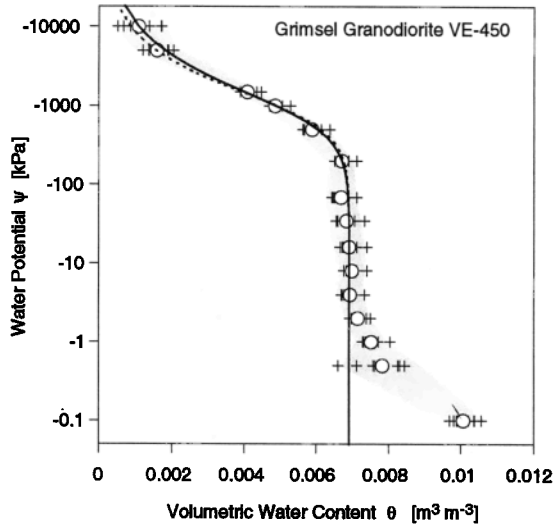

Figure 7. Water retention data of granodiorite samples [*Schneebeli et al.*, 1995]. Mean values of all samples are shown as circles, single observations as crosses. The shaded area encloses two times the standard deviation of the mean volumetric water contents. The solid line is obtained by fitting equation (9) to the data with $\theta_r = 0$ and $\theta_s = 0.0069$ ($\alpha = 1.13$ MPa^{-1}, $n = 1.77$). By fixing θ_s to 0.0069 the data at $\psi \leq 1$ kPa, which were considered as artifacts, were ignored. The dashed line represents the fit obtained from the field-measured water potentials with $\theta_r = 0$ and $\theta_s = 0.0069$ ($\alpha = 1.04$ MPa^{-1}, $n = 1.90$; see text).

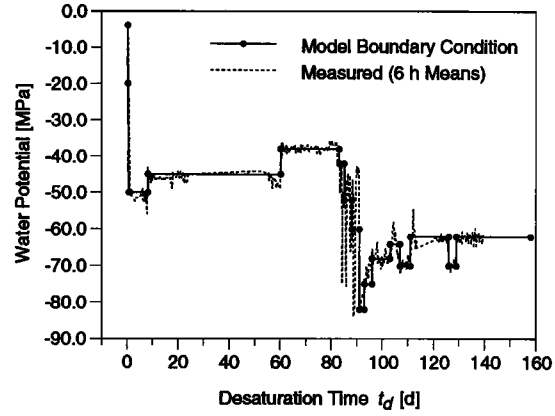

Figure 8. Idealized water potential in the drift (solid line) used as boundary condition for the model compared to the 6-hour means of the measurements (dashed line).

Model calculations were performed for the desaturation phase only, since the water retention data represent a desaturation as well. In Figure 8 the idealized model boundary condition at the drift surface is shown in comparison with the 6-hour averages of the relative humidity measurements. Especially between days 80 and 90, the large scatter in the measurements made it difficult to assign effective mean values. At 400 cm a constant head of 0.06 MPa was assumed according to the observations in piezometer 84018/4 on the opposite side of the tunnel (cf. Figure 5).

A saturated hydraulic conductivity k_s of 3.0×10^{-11} m s^{-1} was estimated for the field site, using the measured water potentials at all depths to calculate the objective function. This k_s value led in general to a satisfactory description of the measured water potentials, as can be seen in Figure 9. It is important to realize that the value of k_s influences only the dynamic response to a change in the tunnel climate, that is, how long it takes until steady state values are achieved. Steady state values themselves do not depend on k_s, but only on the other hydraulic parameters and the boundary conditions.

Under the assumption of normally distributed measurement errors and with a standard deviation of the water potential measurements of 0.05 MPa, the standard error of k_s obtained from the fitting procedure was 5.8×10^{-13} m s^{-1}. This value has to be interpreted with caution, since we do not know how accurate the above assumption is. Estimating k_s from the water potential data at the seven measurement depths separately may illustrate better the possible range of this parameter within the granodiorite matrix. For the individual depths, we obtained k_s values of 2.4×10^{-11} (2 and 5 cm), 4.0×10^{-11} (10

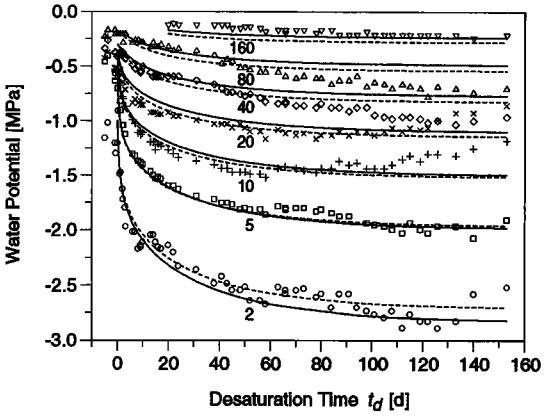

Figure 9. Simulated changes of the water potentials at indicated depths (in centimeters) as compared to the measured reactions. For the solid lines, only the saturated hydraulic conductivity $k_s = 3.0 \times 10^{-11}$ m s^{-1} was estimated from the field-measured water potentials. The dashed lines represent simulations where α, n, and k_s were fitted from the field data.

cm), 6.1×10^{-11} (20 cm), 5.0×10^{-11} (40 cm), 4.4×10^{-11} (80 cm), and 9.8×10^{-12} m s^{-1} (160 cm). There is no obvious trend with the depth in these fitted values.

It is difficult to compare measured and predicted water content changes reliably, since the depth-TDR rods extended over 25 or 30 cm of possibly variably saturated rock, and we do not know exactly how this influences the measurements. In Figure 10 the changes $\Delta\theta$ between actual and initial water content predicted for the different TDR probes with $k_s = 3.0 \times 10^{-11}$ m s^{-1} are shown together with the measurements. The modeled curves were obtained by averaging the water contents calculated at individual nodes, weighted with their element sizes, over the length of the TDR rods or over the first 0.5 cm or the first 5 cm for the surface probe. In general, it seems that the predicted changes are of the same order as the measured ones, except for the surface probe. The measurements did not contradict the predictions at larger depths, although no clear trends towards lower water contents could be observed experimentally at 30–60 and 60–85 cm. At the surface the measured change exceeded the modeled by far. This may be explained by the occurrence of small amounts of liquid water initially on the surface electrode, which evaporated quickly upon start of ventilation. The model, on the other hand, started already from rather low water contents near the surface according to the initial water potentials of about −1 MPa at 2 cm depth (corresponds to a water saturation s_e of about 0.7) or about −4 MPa in the tunnel air ($s_e \approx 0.3$). After 150 days, water saturations $s_e < 0.75$ were calculated for depths $z < 40$ cm, whereas saturations $s_e < 0.5$ were obtained only for $z < 7$ cm. At 160 cm the calculated water saturation after 150 days was about 0.95.

Figure 11 shows the time-dependent density of the water flux into the drift calculated with HYDRUS, using α and n as determined from the laboratory water retention data and k_s as fitted from the field-measured water potential data. The steady state flux value is approximately 2.7×10^{-10} m s^{-1} or 0.023 mm d^{-1}. For the time period between $t_d = 60$ and 150 days, *Bossart et al.* [1994] estimated the water flux from the matrix zone into the drift at the test site indirectly from a ventilation test and from evaporation measurements. They obtained mean values for this time period of 0.048 mm d^{-1} (ventilation test) and 0.026 mm d^{-1} (evaporation measurements), that is, flux densities of the same order of magnitude as the simulated one.

From borehole injection tests in granodiorite at the Grimsel test site [*Heiniger*, 1992], k_s was estimated to lie between 3.8×10^{-12} and 2.2×10^{-10} m s^{-1}. *Kull et al.* [1993] performed ventilation tests in the VE drift, where they measured the water inflow into the drift and the hydraulic gradient between two observation boreholes under varying climatic conditions. They concluded that the large-scale hydraulic conductivity in granodiorite is in the order of 10^{-11} m s^{-1}. *Bossart et al.* [1994] compared the results of evaporation measurements with those of ventilation tests during our desaturation experiment. They derived k_s values of 3.9×10^{-11} m s^{-1} (ventilation test) and 2.1×10^{-11} m s^{-1} (evaporation tests) assuming steady state conditions and a fully saturated rock matrix. It has to be mentioned that these assumptions were obviously inadequate for

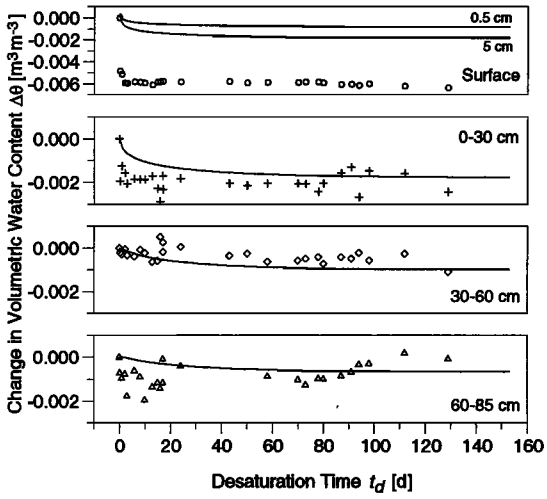

Figure 10. Predicted changes between actual and initial water content for the different TDR sensors (solid lines), based on an estimation of k_s to match measured and calculated water potentials at all depths, as compared to the measured changes (symbols). See section 2.3 for measurement uncertainties.

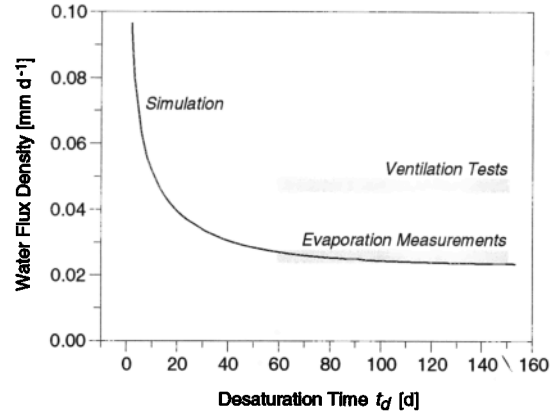

Figure 11. Time dependence of the simulated water flux density across the drift wall during the desaturation phase, based on an estimation of k_s from the field-measured water potentials. The grey bars indicate average values for the period between 60 and 150 days obtained by *Bossart et al.* [1994] from ventilation tests and evaporation measurements.

this time period, which means that the derived k_s values must be interpreted with caution. The values of k_s estimated from our experiments presented in this paper fall well within the range of previously reported values.

Measurements and model calculations, where only the parameter k_s was estimated from part of the field data, seem to agree fairly well in our field study. A simultaneous estimation of α, n, and k_s from the field-measured water potentials led to $\alpha = 1.04$ MPa^{-1}, $n = 1.90$, and $k_s = 2.7 \times 10^{-11}$ m s^{-1}. Model simulations with these optimized parameters are shown as dashed lines in Figure 9. The corresponding water retention function (dashed line in Figure 7) is surprisingly similar to the one fitted from the laboratory measurements, even if we bear in mind that in both cases identical θ_r and θ_s were used. This similarity seems to justify a posteriori the use of small laboratory samples to infer the van Genuchten parameters α and n for the field.

The water transport model is based on a one-dimensional governing equation and neglects the radial symmetry of the experimental domain, thus assuming a constant cross-sectional area. The increase of the cross-sectional area with depth in a radially symmetric, two-dimensional domain would slow down the spreading of a perturbation induced at the tunnel surface, compared with the spreading in a rectangular domain. The effect of the nonconstant area is expected to be minor for the measurement locations between 2 and 40 cm because of the relatively large radius of 1.75 m of the drift, but it might be recognized at 80 and 160 cm. However, the deviations between simulations and measurements show opposite trends at 80 and 160 cm, indicating that the deviations are not linked to the one-dimensional representation of the domain.

When ventilated, the surfaces of the rock matrix looked mostly dry. This suggests that near the tunnel wall, transport of water vapor dominated liquid-phase transport. Therefore the k_s values estimated in this study with a single-phase transport model might be biased by including vapor movement. However, the measured water potentials as well as the calculated water saturations showed relatively steep gradients near the tunnel wall. This limits the zone of dominating vapor transport presumably to the first few centimeters, such that the effect on the estimated k_s value is probably minor.

4. Summary and Conclusions

The direct measurement of water potentials in granitic rock was successfully performed with psychrometers in a field experiment at the Grimsel test site (Central Swiss Alps). The results clearly demonstrated that ventilation of a drift with atmospheric air leads to negative water potentials in the rock, even if the undisturbed hydrostatic pressure within the geological formation is in the order of 3 to 4 MPa. Within half a year, negative potentials were observed up to a distance of 1.6 m from the tunnel wall, which was the largest distance at which a thermocouple psychrometer was installed. The water potential decrease could be reversed by stopping the ventilation. Except near the surface, the water content changes observed with TDR were less pronounced. From the modeling results, it was estimated that at 160 cm the water saturations were still in the order of 0.95 after 150 days of ventilation, and saturations <0.5 were only obtained for $z < 7$ cm.

The temporary occurrence of an unsaturated zone around a ventilated drift has several consequences for the conceptualization of the near field. The hydraulic conductivity k will be radially variable in this case, since it is a function of the water potential, and the flow field around the drift will be different from the one that will develop after closing of the drift. In general, any underground testing during the operation phase should take into consideration the possible presence of an unsaturated zone. In particular, mass balance tests over such tunnel sections, aimed at determining large-scale macropermeabilities, should be interpreted accordingly. The present experiments suggest that the desaturation is reversible and the near field can reach its fully saturated state, some time after sealing.

Our desaturation measurements could be modeled quite successfully with a one-dimensional, single-phase water flow model (HYDRUS 5.0 [*Vogel et al.*, 1996]) by using the van Genuchten parameters inferred from laboratory water retention data ($\alpha = 1.13$ MPa^{-1}, $n = 1.77$, $\theta_s = 0.0069$, and $\theta_r = 0$) and by estimating a depth-invariant saturated hydraulic conductivity, k_s. Using the measured water potentials at all depths in the objective function, we obtained $k_s = 3.0 \times 10^{-11}$ m s^{-1}. Using only water potentials at a single depth led to the following k_s values: 2.4×10^{-11} (2 and 5 cm), 4.0×10^{-11} (10 cm), 6.1×10^{-11} (20 cm), 5.0×10^{-11} (40 cm), 4.4×10^{-11} (80 cm), and 9.8×10^{-12} m s^{-1} (160 cm). The estimated k_s values are in the range of previously reported values for the granodiorite matrix. To judge whether the moisture capacity $C(\psi)$ as obtained from the water retention curve of small samples is appropriate for the field situation, it is important to compare not only modeled and measured water potentials, but also the corresponding water contents. In our case the predicted water content changes were relatively small, which agreed with the measurements at larger depths. The initial difference at the surface can possibly be explained by a discrepancy between the modeled and measured initial condition.

If a tunnel segment is ventilated, water vapor transport will certainly be of importance. The fact that a single liquid-phase transport model could describe the measured desaturation at depths larger than 2 cm more or less adequately indicates, however, that vapor phase transport is relevant only within the first few centimeters adjacent to the tunnel wall, where water saturations lower than 0.5 occur during ventilation.

Local structural properties can influence the temporal reactions of the water potential to ventilation, as can be seen from the measurements at 10 and 20 cm for $t_d > 120$ days or in general from the variation of the fitted k_s for the various depths. The predictive capability of a model will therefore strongly depend on the accuracy of the used parameter set and of the boundary representations for the modeled domain, which is of course closely related to the problem of spatial parameter variations.

Acknowledgments. These investigations were funded by Nagra, the National Cooperative for the Disposal of Radioactive Waste, Switzerland, and by the ETH Zürich (Cooperative Research Program "Water transport in unsaturated granite rock matrix"). We would like to thank B. Frieg and S. Vomvoris (Nagra) for the professional and encouraging management of the Cooperative Research Program, W. Kickmaier and H. Abplanalp (Nagra) for their valuable on-site support, E. Meier (Meier & Partners, Winterthur, Switzerland) for providing independently measured relative humidity data, and H. Kull (GRS, Braunschweig, Germany) for making the piezometer data of the boreholes 84011 and 84018 available to us. We acknowledge also the very helpful review by W. N. Herkelrath.

References

Bossart, P., Geological and structural characterization of the ventilation test site, in Overview of Nagra field and modeling activities in

the ventilation drift (1988–1990), edited by S. Vomvoris and B. Frieg, *Nagra Tech. Rep. NTB 91-34*, Nagra, Wettingen, Switzerland, 1992.

Bossart, P., J. Lang, and U. Raz, Water balance in tunnel sections, in Investigation of hydraulic parameters in the saturated and unsaturated zone of the ventilation drift, edited by B. Frieg and S. Vomvoris, *Nagra Tech. Rep. NTB 93-10*, Nagra, Wettingen, Switzerland, 1994.

Durner, W., Hydraulic conductivity estimation for soils with heterogeneous pore structure, *Water Resour. Res.*, *30*, 211–223, 1994.

Heiniger, P., Active and passive hydrogeological testing in the VE drift, in Overview of Nagra field and modeling activities in the ventilation drift (1988–1990), edited by S. Vomvoris and B. Frieg, *Nagra Tech. Rep. NTB 91-34*, Nagra, Wettingen, Switzerland, 1992.

Keusen, H. R., J. Ganguin, P. Schuler, and M. Buletti, Grimsel Test Site–Geology, *Nagra Tech. Rep. NTB 87-14E*, Nagra, Wettingen, Switzerland, 1989.

Kull, H., W. Brewitz, and K. Klarr, Ventilationstest, In-Situ-Verfahren zur Permeabilitätsbestimmung im Kristallin, *Nagra Tech. Rep. NTB 91-02*, Nagra, Wettingen, Switzerland, 1993.

Mualem, Y., A new model for predicting the hydraulic conductivity of unsaturated porous media, *Water Resour. Res.*, *12*, 513–522, 1976.

Press, W. H., S. A. Teukolsky, W. T. Vetterling, and B. P. Flannery, *Numerical Recipes: The Art of Scientific Computing*, 2nd ed., Cambridge Univ. Press, New York, 1992.

Rawlins, S. L., and G. S. Campbell, Water potential: Thermocouple psychrometry, in *Methods of Soil Analysis*, part 1, *Physical and Mineralogical Methods*, *Agron. Monogr.*, vol. 9, edited by A. Klute, pp. 597–618, Soil Sci. Soc. of Am., Madison, Wis., 1986.

Roth, K., R. Schulin, H. Flühler, and W. Attinger, Calibration of time domain reflectometry for water content measurement using a composite dielectric approach, *Water Resour. Res.*, *26*, 2267–2273, 1990.

Schneebeli, M., H. Flühler, T. Gimmi, H. Wydler, H.-P. Läser, and T. Baer, Measurements of water potential and water content in unsaturated crystalline rock, *Water Resour. Res.*, *31*, 1837–1843, 1995.

van Genuchten, M. T., A closed form equation for predicting the hydraulic conductivity of unsaturated soils, *Soil Sci. Soc. Am. J.*, *44*, 892–898, 1980.

Vogel, T., K. Huang, R. Zhang, and M. T. van Genuchten, The HYDRUS code for simulating one-dimensional water flow, solute transport, and heat movement in variably-saturated media, *Res. Rep. 140*, U.S. Salinity Lab., U.S. Dep. of Agric., Riverside, Calif., 1996.

T. Baer, Nagra, Hardstrasse 73, CH-5430 Wettingen, Switzerland.

H. Flühler, T. Gimmi, and H. Wydler, Soil Physics, Institute of Terrestrial Ecology, Swiss Federal Institute of Technology, ETHZ, Grabenstrasse 3, CH-8952 Schlieren, Switzerland. (email: gimmi@ito.umnw.ethz.ch)

M. Schneebeli, Swiss Federal Institute of Snow and Avalanche Research, Davos, Switzerland.

(Received September 23, 1996; revised December 23, 1996; accepted December 23, 1996.)